Dinaciclib (SCH 727965), a Novel and Potent Cyclin-Dependent Kinase Inhibitor

David Parry[1], Timothy Guzi[2], Frances Shanahan[1], Nicole Davis[1], Deepa Prabhavalkar[1], Derek Wiswell[1], Wolfgang Seghezzi[1], Kamil Paruch[2], Michael P. Dwyer[2], Ronald Doll[2], Amin Nomeir[2], William Windsor[2], Thierry Fischmann[2], Yaolin Wang[2], Martin Oft[1], Taiying Chen[1], Paul Kirschmeier[2], and Emma M. Lees[1]

Abstract

Cyclin-dependent kinases (CDK) are key positive regulators of cell cycle progression and attractive targets in oncology. SCH 727965 inhibits CDK2, CDK5, CDK1, and CDK9 activity *in vitro* with IC_{50} values of 1, 1, 3, and 4 nmol/L, respectively. SCH 727965 was selected as a clinical candidate using a functional screen *in vivo* that integrated both efficacy and safety parameters. Compared with flavopiridol, SCH 727965 exhibits superior activity with an improved therapeutic index. In cell-based assays, SCH 727965 completely suppressed retinoblastoma phosphorylation, which correlated with apoptosis onset and total inhibition of bromodeoxyuridine incorporation in >100 tumor cell lines of diverse origin and background. Moreover, short exposures to SCH 727965 were sufficient for long-lasting cellular effects. SCH 727965 induced regression of established solid tumors in a range of mouse models following intermittent scheduling of doses below the maximally tolerated level. This was associated with modulation of pharmacodynamic biomarkers in skin punch biopsies and rapidly reversible, mechanism-based effects on hematologic parameters. These results suggest that SCH 727965 is a potent and selective CDK inhibitor and a novel cytotoxic agent. *Mol Cancer Ther; 9(8); 2344–53. ©2010 AACR.*

Introduction

The mammalian cell cycle is a nonredundant process that integrates extracellular signaling, DNA synthesis, and mitosis (1, 2). Dysregulation of cell cycle control is a hallmark of all human cancers and is frequently associated with selective, aberrant activation of cyclin-dependent kinases (CDK; refs. 3, 4). Several members of the CDK family are critical regulators of cell cycle progression. CDK2 and CDK1 are two closely related kinases that play overlapping roles during cell division, contributing to the phosphorylation and inactivation of the retinoblastoma (Rb) tumor suppressor gene product throughout late G_1, S, and G_2-M phases (5–7). Other CDK family members play important roles outside of direct regulation of cell cycle progression. For instance, CDK7, CDK8, and CDK9 contribute to the regulation of RNA polymerase II and the control of cellular transcription (8, 9).

Inhibition of CDK activities represents an attractive therapeutic strategy in oncology. Indeed, expression of dominant-negative forms of CDK2 or combinatorial silencing of CDK1 and CDK2 through small interfering RNA generates therapeutically relevant phenotypes, such as cell cycle arrest (10–12). Suppression of CDK9 using RNAi has desirable therapeutic effects *in vitro* (13). Similarly, inhibition of CDK9 and the subsequent suppression of MCL1 transcription are proposed as a potential mechanism-of-action for the pan-CDK inhibitor flavopiridol in chronic lymphocytic leukemia (14, 15). Finally, CDK8 is a key modulator of β-catenin function, and the *CDK8* gene is amplified in some human colorectal cancers (16, 17). Furthermore, the lack of appropriate cell cycle regulation in tumor cells predicts their increased propensity for apoptosis, compared with normal tissue (18).

Based on the intriguing and multifaceted attributes of the CDK target class, several small-molecule CDK inhibitors have entered clinical development (19). However, due to the high degree of structural homology within the CDK protein family, putative small-molecule CDK inhibitors may exert their effects through combinatorial inhibition of multiple CDKs and other closely related serine/threonine kinases. Hence, the almost inevitable multitargeted nature of CDK inhibitors places a high premium on maintaining an adequate therapeutic index *in vivo*. A critical issue for the successful development of

Authors' Affiliations: [1]Merck Research Laboratory-Palo Alto, Palo Alto, California and [2]Merck Research Laboratory-Kenilworth, Kenilworth, New Jersey

Note: Supplementary material for this article is available at Molecular Cancer Therapeutics Online (http://mct.aacrjournals.org/).

Current address for T. Guzi: Merck Research Laboratory-Cambridge, 320 Bent Street, Cambridge, MA 02141.

Current address for K. Paruch: Masaryk University, Kamenice 5, 625 00 Brno, Czech Republic.

Current address for E. Lees: Novartis Institutes for Biomedical Research, 4560 Horton Street, Emeryville, CA 94608-2916.

Corresponding Author: David Parry, Merck Research Laboratory-Palo Alto, 901 California Avenue, Palo Alto, CA 94304-1104. Phone: 650-4966524; Fax: 650-4961200. E-mail: david.parry@merck.com

doi: 10.1158/1535-7163.MCT-10-0324

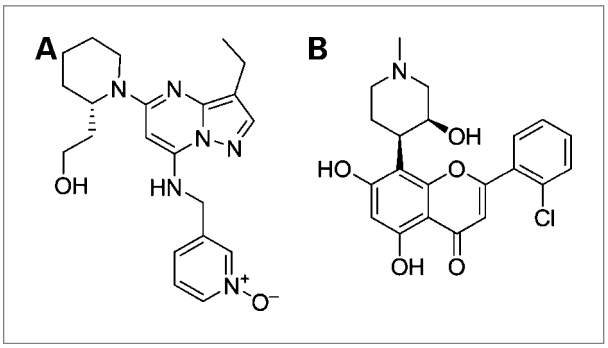

Figure 1. Structures of SCH 727965 (A) and flavopiridol (B).

CDK inhibitors (and indeed the majority of cytoreductive agents) is, therefore, the relationship between desirable, target-specific effects and the onset of nonspecific adverse events that might negatively influence clinical dose escalation (20). Selection of Dinaciclib (SCH 727965; Fig. 1A) for clinical development was facilitated by a range of diverse assays and included an *in vivo* screening strategy that identified candidate compounds with the optimal combination of pharmacokinetic, efficacy, and safety characteristics (21). This highly effective, functional approach allowed for rapid benchmarking against known CDK inhibitors with undesirable side effects, such as flavopiridol (Fig. 1B), and showed SCH 727965 to be a compound with a significantly superior therapeutic profile.

Materials and Methods

Experimental and control agents

SCH 727965 (*(S)*-(−)-2-(1-{3-ethyl-7-[(1-oxy-pyridin-3-ylmethyl)amino] pyrazolo[1,5-a]pyrimidin-5-yl} piperidin-2-yl)ethanol) and flavopiridol (2-(2-chlorophenyl)-5,7-dihydroxy-8-[(3S,4R)-3-hydroxy-1-methyl-4-piperidinyl]-4-chromenone) were supplied by Schering-Plough Research Institute. Paclitaxel was purchased from Sigma. The vehicle for these agents, except paclitaxel, was 20% hydroxypropyl-β-cyclodextran. The vehicle for paclitaxel was Cremophor. Dosing volume was 0.2 mL per injection.

Cyclin/CDK kinase assay

Recombinant cyclin/CDK holoenzymes were purified from Sf9 cells engineered to produce baculoviruses that express a specific cyclin or CDK. Cyclin/CDK complexes were typically diluted to a final concentration of 50 μg/mL in a kinase reaction buffer containing 50 mmol/L Tris-HCl (pH 8.0), 10 mmol/L $MgCl_2$, 1 mmol/L DTT, and 0.1 mmol/L sodium orthovanadate. For each kinase reaction, 1 μg of enzyme and 20 μL of a 2-μmol/L substrate solution (a biotinylated peptide derived from histone H1; Amersham) were mixed and combined with 10 μL of diluted SCH 727965. The reaction was started by the addition of 50 μL of 2 μmol/L ATP and 0.1 μCi of ^{33}P-ATP (Amersham). Kinase reactions were incubated for 1 hour at room temperature and were stopped by the addition of 0.1% Triton X-100, 1 mmol/L ATP, 5 mmol/L EDTA, and 5 mg/mL streptavidin-coated SPA beads (Amersham). SPA beads were captured using a 96-well GF/B filter plate (Packard/Perkin-Elmer Life Sciences) and a Filtermate universal harvester (Packard/Perkin-Elmer Life Sciences.) Beads were washed twice with 2 mol/L NaCl and twice with 2 mol/L NaCl containing 1% phosphoric acid. The signal was then assayed using a TopCount 96-well liquid scintillation counter (Packard/Perkin-Elmer Life Sciences). Dose-response curves were generated from duplicate, eight-point serial dilutions of inhibitory compounds. IC_{50} values were derived by nonlinear regression analysis.

Kinase counter-screening

SCH 727965 and flavopiridol were counter-screened using the Millipore Kinase Profiler service. Both compounds were tested at 1.0 and 10.0 μmol/L against a panel of diverse kinases, using a fixed (10 μmol/L) concentration of ATP.

Cell lines and cell culture

The majority of the tumor cell lines were obtained from the American Type Culture Collection and propagated under the suggested growth conditions. Mantle cell lymphoma cell lines were generously provided by Dr. Geoffrey Shapiro (Dana-Farber Cancer Institute, Boston, MA).

dThd uptake growth inhibition assay

A2780 cells were maintained in DMEM (Cellgro) plus 10% fetal bovine serum (HyClone) and passaged twice weekly by detaching the monolayer with trypsin-EDTA (Life Technologies). One hundred microliters of A2780 cells (5×10^3 cells) were added per well to a 96-well Cytostar-T plate (Amersham) and incubated for 16 to 24 hours at 37°C. Compounds were serially diluted in complete media plus 2% ^{14}C-labeled dThd (Amersham). Media were removed from the Cytostar T plate; 200 μL of various compound dilutions were added in quadruplicate; and the cells were incubated for 24 hours at 37°C. Accumulated incorporation of radiolabel was assayed using scintillation proximity and measured on a TopCount (Packard/Perkin-Elmer Life Sciences). The percentage of dThd uptake inhibition, relative to a vehicle control, was calculated and plotted on log-linear plots to allow derivation of IC_{50} values.

Bromodeoxyuridine incorporation assay

A2780 cells were plated into six-well tissue culture dishes and allowed to adhere. Cells were then exposed to differing concentrations of SCH 727965 or a DMSO control vehicle for 24 hours, followed by a brief (30 min) pulsed exposure to bromodeoxyuridine (BrdUrd). Cells were then harvested, immunostained

using FITC-conjugated antibodies specific for BrdUrd (BD Biosciences), counter-stained with propidium iodide/RNase A solution (BD Biosciences), and analyzed using flow cytometry. Fluorescence-activated cell sorting analyses were done on a FACSCalibur instrument (Becton Dickinson). FITC-positive BrdUrd staining and propidium iodide signal allowed assessment of ongoing DNA replication and the cell cycle stage. Percentages of the cell population in each cell cycle stage were plotted for each test article concentration.

Immunoblotting

Asynchronously growing tumor cell lines were exposed to differing concentrations of SCH 727965. Subsequently, cells were harvested and lysed in a 50 mmol/L Tris-HCl buffer containing 350 mmol/L NaCl, 0.1% NP40, 1 mmol/L DTT, and a cocktail of protease and phosphatase inhibitors (Calbiochem). Following protein concentration determination (Bio-Rad), cell lysates were separated on reducing SDS-PAGE gels and immunoblotted with antisera specific for Rb phosphorylated on serines 807, 811 (Cell Signaling), hypophosphorylated Rb (Cell Signaling), or the p85 poly ADP ribose polymerase (PARP) caspase cleavage product (Promega).

Induction of apoptosis assessed by activated caspase

Assays of caspase activation were done using the Beckman Coulter CellProbe HT Caspase-3/7 Whole Cell Assay system. Asynchronously growing cells were plated into 96-well plates and allowed to adhere. Cells were exposed to differing concentrations of SCH 727965 or vehicle for 24 hours. Cells were subsequently incubated with a fluorescently labeled caspase substrate (CellProbe); uptake and fluorescence of the substrate within cells correlate with the level of activated caspases. The caspase activity was determined using an Analyst AD 96.384 fluorometer (485 nm excitation and 530 nm emission).

Clonogenicity and alamarBlue viability assays

Cells were plated onto tissue culture dishes and propagated with the appropriate growth media. Growing cultures were exposed to increasing concentrations of SCH 727965 or a vehicle control, typically for 7 days. After removing the medium, cells were fixed with 50% methanol/50% acetone for 5 minutes and stained with 0.2% crystal violet (Fisher) in 2% ethanol for 5 minutes. Following staining, cells were washed with 5 to 10 mL of water. Stained cells were solubilized in 1% deoxycholic acid (Sigma), and the absorbance of the resulting solution was measured at 600 nm using a SOFTmax PRO 4.3 plate reader (Molecular Devices). Absorbance of SCH 727965–treated samples was plotted as a percent of that of a vehicle-treated control, and data were reported as an IC_{50} value relative to these controls. For suspension cell lines, assessments of cell viability were obtained using the alamarBlue Cell Viability Assay kit (Biotium), using the manufacturers' recommended protocol.

Experimental mice

All mouse strains were obtained from Charles River Laboratories. Female nude mice age 9 to 14 week or female BALB/c mice age 6 to 14 weeks were used. Animals were housed in an Association for Assessment and Accreditation of Laboratory Animal Care-accredited animal facility at Schering-Plough Biopharma, Palo Alto, CA, and Schering-Plough Research Institute, Kenilworth, NJ. Conventional animal chow and water were provided *ad libitum*. All protocols related to experiments using animals have been approved by the appropriate Institutional Animal Care and Use Committee.

In vivo tumor growth assessments

For tumor implantation, specific cell lines were grown *in vitro*, washed once with PBS, and resuspended in 50% Matrigel (BD Biosciences) in PBS to a final concentration of 4×10^7 to 5×10^7 cells per milliliter. Nude mice were injected with 0.1 mL of this suspension s.c. in the flank region. Tumor length (L), width (W), and height (H) were measured by a caliper twice weekly on each mouse and then used to calculate tumor volume using the formula $(L \times W \times H)/2$. When the tumor volume reached ~100 mm^3, the animals were randomized to treatment groups (10 mice/group) and treated i.p. with either SCH 727965 or individual chemotherapeutic agents according to the dosing schedule indicated in table and figure legends. Tumor volumes and body weights were measured during and after the treatment periods. Data were expressed as means ± SEM. Animals were euthanized according to the Institutional Animal Care and Use Committee guidelines.

Immunohistochemical staining of phospho-Rb protein

Samples were harvested from the nude mice skin at various time points following administration of a single 40-mg/kg dose of SCH 727965. The samples were fixed overnight in 10% formaldehyde, washed in 70% ethanol, and processed in a tissue processor (Thermo Electronic Co.); the tissues were dehydrated in graded ethanol solutions, cleared in three changes of xylene, and penetrated in heated paraffin (at 56–58°C). The tissues were embedded in paraffin, cut into 4- to 6-μm sections, and placed onto slides. Before staining, the slides were placed in a chamber containing 1× Reveal Solution (BioCare Medical) for deparaffinization and antigen retrieval. The slides were rinsed in hot water, placed in PBS for 15 minutes at room temperature, and loaded onto a DAKO automated immunostainer. Endogenous hydrogen peroxidase activity was blocked with hydrogen peroxide for 10 minutes followed by rinsing with a Tris-HCl buffered saline solution containing 0.5% Tween 20 (TBST; Sigma). The slides were then sequentially incubated with avidin, rinsed in TBST, treated with biotin, and rinsed again in TBST (avidin/biotin block kit; Vector Laboratories). Nonspecific binding sites were blocked with 1× blocking buffer (Sigma) for 20 minutes. The slides were then incubated

with anti-phospho Rb 807/811 (Cell Signaling) diluted 1:75 or rabbit control antisera at 1 μg/mL for 45 minutes, rinsed with TBST, and incubated with biotinylated goat anti-rabbit IgG (Elite ABC kit; Vector Laboratories) for 30 minutes. The slides were rinsed again with TBST and treated with ABC complex (Elite ABC kit; Vector Laboratories) for 30 minutes, followed by another TBST rinse. The slides were developed in 3,3′-diaminobenzidine (Dakocytomation) for 5 minutes, rinsed with TBST, and incubated for 2 minutes with hematoxylin (Dakocytomation). Finally, the slides were rinsed in distilled water, dehydrated in graded ethanol solutions, cleared in xylene using a Leica autostainer, and cover slipped in a Leica Cover slipper.

Assessments of SCH 727965 effects on hematologic parameters

A daily dose of SCH 727965 (40 mg/kg) was administered i.p. to BALB/c mice for 5 days. Blood was collected on day 6 and day 13 (1st and 7th day after the final dose, respectively), diluted 1:5 in PBS, and immediately analyzed on an Advia 120 hematology analyzer (with differential).

Pharmacokinetic determinations

Plasma samples from mice were collected at various times after i.p. administration of SCH 727965. At each time point, blood samples from three animals were combined and analyzed for SCH 727965 by liquid chromatography-tandem mass spectrometry. Pharmacokinetic variables were estimated from the plasma concentration data. Maximum plasma concentration values were taken directly from the plasma concentration time profiles, and the area under the plasma concentration versus time curve (0–24 h) was calculated using the linear trapezoidal rule.

Results

SCH 727965 selection using a mouse tumor xenograft model

SCH 727965 was selected as the optimal drug candidate for clinical development by screening individual, diversely substituted compounds against the A2780 ovarian carcinoma mouse xenograft model, using flavopiridol as a benchmark control agent. This system established the ratio of maximum tolerated dose (MTD) and minimum effective dose (MED) for each tested compound. MTD was determined following i.p. administration of each compound to nude mice at varying dose levels once daily for 7 days and defined as the dose associated with a body weight reduction of 20%. In parallel, MED was defined as the dose, given by the same schedule, associated with >50% tumor growth inhibition. Promising compounds were further profiled in rats and dogs (21). The screening data pertinent to SCH 727965 are outlined in Table 1. Thus, MTD and MED of SCH 727965 were >60 and 5 mg/kg, respectively; in contrast, MTD and MED of flavopiridol were <10 and 10 mg/kg, respectively. Therefore, a screening therapeutic index (MTD/MED ratio) of SCH 727965 was >10, whereas the index of flavopiridol was <1, indicating that minimal antitumor efficacy was not attained with flavopiridol before the onset of dose-limiting toxicity. These data indicated that SCH 727965 has an attractive *in vivo* profile that is superior to flavopiridol.

SCH 727965 is a potent and selective inhibitor of CDKs

Inhibition of the kinase activity of various cyclin/CDKs was examined using isolated, baculovirus-expressed holoenzymes *in vitro*. SCH 727965 inhibits CDK2, CDK5, CDK1, and CDK9 with IC_{50} values of 1, 1, 3, and 4 nmol/L, respectively. Compared with flavopiridol and assayed under identical conditions, SCH 727965 is an equally potent inhibitor of CDK1 and CDK9 but a 12- and 14-fold stronger inhibitor of CDK2 and CDK5, respectively (Table 1). SCH 727965 was found to be a potent DNA replication inhibitor that blocked thymidine (dThd) DNA incorporation in A2780 cells with an IC_{50} of 4 nmol/L. In contrast, flavopiridol had an ~16-fold lesser potency in that assay. These data show that SCH 727965's stronger and more selective inhibition of CDKs translates into its more potent inhibition of DNA synthesis compared with flavopiridol in cell-based assays (Table 1).

SCH 727965 is not a general kinase inhibitor (Supplementary Table S1) and, in a series of additional kinase

Table 1. Comparison between SCH 727965 and flavopiridol: inhibition of CDKs, dThd incorporation, and activity in a mouse tumor xenograft

Compound	CDK2	CDK5	CDK1	CDK9	dThd incorporation	MTD*	MED†	(MTD/MED)‡
	IC_{50} (nmol/L)					(mg/kg)		
SCH 727965	1	1	3	4	4	60	5	>10
Flavopiridol	12	14	3	4	70	<10	10	<1

*MTD: 20% weight loss.
†MED: >50% inhibition of tumor growth (both administered i.p. once daily for 7 d).
‡Screening therapeutic index.

Table 2. Millipore kinase profiler counter-screening for SCH 727965 and flavopiridol

Kinase	SCH 727965		Flavopiridol	
	1 μmol/L	10 μmol/L	1 μmol/L	10 μmol/L
	Kinase activity remaining (%)			
AMPK	94	62	67	20
Blk	69	100	73	26
CaMKII	102	91	44	30
CDK6/cyclin D3	12	3	25	6
CDK7/cyclin H1/MAT1	7	4	16	6
c-Src	117	111	3	4
Fes	87	91	44	13
Lyn	108	110	73	18
MSK1	94	97	74	37
PKC α	96	94	65	20
PKC β II	110	113	75	26
PKC ε	93	88	45	9
PKC θ	95	95	23	5
RSK2	104	76	65	16
Yes	92	98	68	40

counter-screens (Table 2), was shown to be more selective or the CDK family, compared with flavopiridol. These data showed that flavopiridol affects a broader range of serine/threonine and tyrosine kinases (e.g., c-Src), which may contribute to its poor screening therapeutic index compared with that of SCH 727965.

SCH 727965 inhibits phosphorylation of the Rb tumor suppressor protein and induces accumulation of the p85 PARP caspase cleavage product

Inhibition of CDK-specific serine 807 and 811 (Ser 807/811) phosphorylation on the Rb tumor suppressor protein and accumulation of p85 PARP caspase cleavage product (p85 PARP) were selected as mechanism-based markers. These were used to explore the mechanism of dThd uptake inhibition observed upon cell exposure to SCH 727965 or flavopiridol, and correlate onset of apoptosis with inhibition of CDKs (Fig. 2). Lysates from asynchronously growing A2780 cells treated with increasing concentrations of SCH 727965 or flavopiridol for 16 hours were analyzed on SDS-PAGE and immunoblotted with Ser 807/811 Rb–specific antisera or with p85 PARP-specific antisera.

SCH 727965 strongly suppressed phosphorylation of Rb on Ser 807/811 at concentrations >6.25 nmol/L, which is in accord with the observation that 4 nmol/L concentrations are required for 50% inhibition of dThd DNA incorporation in the same cell model as previously described. Significantly, complete suppression of Rb phosphorylation was correlated with the onset of apoptosis, as indicated by the appearance of the p85 PARP cleavage product in cells exposed to >6.25 nmol/L SCH 727965 (Fig. 2A, left). No evidence of apoptosis induction was detectable before the complete suppression of Rb phosphorylation. In contrast, flavopiridol was less effective at inducing significant suppression of Rb phosphorylation, and concentrations approaching 1 μmol/L were required to induce detectable effects on phospho-Rb Ser 807/811 levels (Fig. 2A, right). Of note, flavopiridol stimulated the accumulation of the p85 PARP cleavage product concentrations otherwise insufficient to inhibit Rb phosphorylation, suggesting a poor correlation between flavopiridol-induced apoptosis and Rb phosphorylation status. In contrast, the cytotoxic activity of SCH 727965 and its effect on Rb phosphorylation correlate with its proposed mechanism of action based on selective inhibition of CDKs.

Mechanism of action-based effects following a short cellular SCH 727965 exposure

To determine whether short exposures to SCH 727965 were able to induce responses similar to those following 16- to 24-hour exposures described above, A2780 cells were treated with 100 nmol/L SCH 727965 for 2 hours, washed out and supplied with a drug-free medium. Cell lysates from a time course of 2-hour intervals were then separated on SDS-PAGE and immunoblotted with antisera specific for hypophosphorylated Rb and p85 PARP; this allowed the assessment of CDK inhibition and apoptosis activation. A 2-hour exposure to 100 nmol/L SCH 727965 was sufficient to induce suppression of Rb phosphorylation and caspase activation, detectable up to 6 hours later (Fig. 2B). Induction of apoptosis was confirmed using a quantitative, fluorometric cell-based assay of caspase activation following short exposures to as little as 50 nmol/L of SCH 727965 (Fig. 2C).

To examine the effects of a short SCH 727965 exposure on cell cycle, asynchronously growing A2780 cells treated with increasing concentrations of SCH 727965 for 2 hours were maintained for 24 hours in a drug-free medium, then pulse labeled with BrdUrd to establish the percentage of cells undergoing active DNA replication, before analysis by fluorescence-activated cell sorting. Under these conditions, cells exposed to 125 to 250 nmol/L SCH 727965 for 2 hours partially suppressed DNA synthesis and BrdUrd incorporation for 24 hours (Fig. 2D). Higher exposures (≤500 nmol/L) were sufficient to completely suppress DNA synthesis for 24 hours and were correlated with the accumulation of apoptotic (sub-G_1) cells. Overall, these data show that short exposures to SCH 727965 can induce long-lasting effects in target cells and imply that continuous exposure to SCH 727965 may not be required for sustained activity *in vivo*.

SCH 727965 activity in a panel of tumor cell lines

CDK inhibitors are expected to have broad antiproliferative activity against a wide range of tumor cells. SCH 727965 antiproliferative activity (clonogenicity, alamarBlue viability assay, dThd and BrdUrd incorporation,

and p85 PARP marker analysis) was examined in an extended panel of human tumor cell lines that included the full NCI-60 screening set and an additional 47 cell lines procured to expand representation of small-cell lung cancer, lymphoma, leukemia, prostate, and pancreatic cancers. The broad range of transformed cellular backgrounds (p53, pRB, p16, c-Myc, K-Ras, etc.) allowed SCH 727965 testing in diverse settings. Tumor cell line origin and response characteristics are summarized in Table 3.

The mean and median IC_{50} values across this cell line panel were 10 and 11 nmol/L, respectively. Complete suppression of BrdUrd incorporation in the tested cell lines was typically apparent at concentrations that induce inhibition of clonogenicity by 90% (20–25 nmol/L; data not shown). Following exposure to SCH 727965, all tested human tumor cell lines underwent cell cycle arrest, and no selectivity toward a specific tumor type was observed. Furthermore, apoptosis, which was determined by the appearance of the p85 PARP cleavage product on Western blots following a single exposure to SCH 727965 at concentrations <100 nmol/L, was detected in >85% of the cell lines tested. Approximately 50% of cell lines from the NCI-60 screening panel express multiple drug resistance gene 1, and it is noteworthy that multiple drug resistance gene 1 status did not

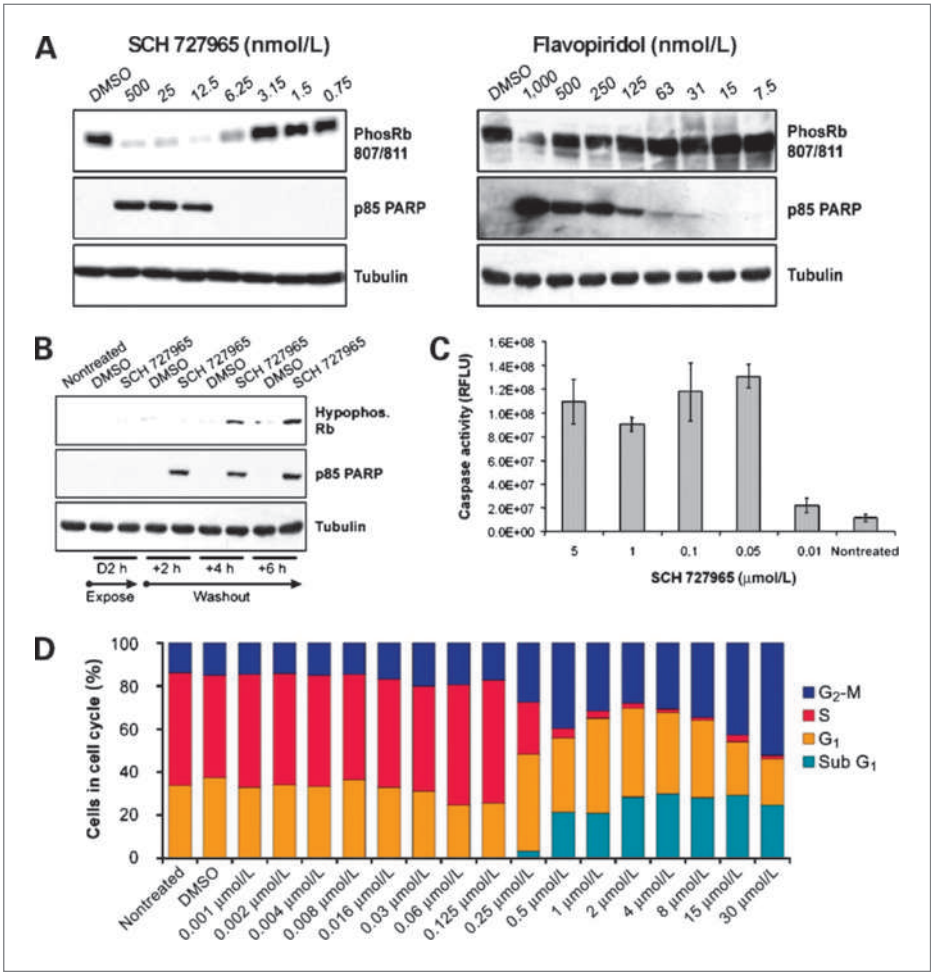

Figure 2. Mechanism-based marker analyses in human cancer cells. A, asynchronously growing A2780 cells were treated for 16 h with increasing concentrations of SCH 727965 (left) or flavopiridol (right), as indicated. Cell lysates were immunoblotted with anti-phospho Rb 807/811, a marker of cellular CDK activity, anti-p85 PARP caspase cleavage product, a marker indicating activation of caspases, and anti-tubulin, a loading control. B, short treatment with SCH 727965 induces mechanism-based effects in human cancer cells. Lysates from asynchronously growing A2780 cells exposed to 100 nmol/L SCH 727965 for 2 h were separated on PAGE-SDS and immunoblotted with antisera specific for hypophosphorylated Rb, p85 PARP caspase cleavage product, and tubulin as a control. C, caspase activation analysis using a quantitative fluorometric analysis. A2780 cells were exposed to increasing concentrations of SCH 727965, as indicated, for 2 h, and analyzed 6 h after the drug washout. Caspase activation was observed following exposure to 50 nmol/L of SCH 727965 and did not increase with elevated levels of SCH 727965 (up to 5 μmol/L). D, cell cycle distribution following short treatment with SCH 727965. Asynchronously growing A2780 cells were exposed to increasing concentrations of SCH 727965 for 2 h, cultured for an additional 24 h in drug-free medium, and then pulsed for 30 min with BrdUrd. A 2-h exposure to ≤500 μmol/L SCH 727965 was sufficient to suppress >90% of BrdUrd incorporation 24 h later.

Table 3. SCH 727965 is active against a broad spectrum of human tumor cell lines

Tumor cell line	Mean in-cell IC_{50} (clonogenicity; nmol/L)	Detectable caspase activation* (single exposure)
Prostate	12	4 of 5
Breast	8	6 of 7
Colon	17	5 of 9
SCLC	14	8 of 9
SCLC	6	2 of 6
Ovarian	14	5 of 7
Pancreatic	15	11 of 15
Melanoma	9	9 of 9
Leukemia	6	5 of 6
Bladder	10	1 of 2
Liver	8	2 of 2
Mantle cell lymphoma	7	3 of 4
Lymphoma (NHL)	7	8 of 8

Abbreviations: SCLC, small-cell lung cancer; NHL, non-Hodgkin lymphoma.

*Data indicate the number of caspase-positive cell lines out of total number of cell lines from each tumor cell line type tested.

significantly influence sensitivity to SCH 727965. Overall, these data suggest that SCH 727965 has antiproliferative activity across a broad range of tumor types and genetic backgrounds.

SCH 727965 efficacy and tolerability *in vivo*

The previously described A2780 ovarian cancer mouse xenograft model developed for initial selection of active agents was used for further assessment of SCH 727965 efficacy and tolerability; paclitaxel was a positive control. Nude mice with ~100 mm^3 A2780 tumors were randomized into groups of 10 animals ~7 days after initial s.c. cell inoculation and assigned to each SCH 727965 dosage group, paclitaxel, or vehicle control. SCH 727965 i.p. administration at 8, 16, 32, and 48 mg/kg daily for 10 days resulted in tumor inhibition by 70%, 70%, 89%, and 96%, respectively; paclitaxel i.p. administration at 20 mg/kg twice weekly inhibited tumor growth by 63% (Fig. 3A). Consistent with earlier *in vivo* screening data, SCH 727965 MED appears to be <8 mg/kg. SCH 727965 was well tolerated, and the maximum body weight loss in the highest dosage group was 5% (data not shown). This is well below the MTD defined as 20% loss of body weight over the course of this experiment. Taken together, the data show that SCH 727965 has dose-dependent antitumor activity *in vivo*, and that nearly complete inhibition of tumor growth occurs at a dose level below the MTD (Table 4; Fig. 3A).

SCH 7279765 has antitumor activity on various intermittent schedules

Pharmacokinetic studies showed that SCH 727965 has a short plasma half-life in mouse. Thus, a dose of 5 mg/kg SCH 727965 given i.p. in mice was associated with a plasma half-life of ~0.25 hour (Supplementary Table S2), perhaps suggesting a need for frequent dosing. However, previous results imply that continuous SCH 727965 exposure may not be a prerequisite for antiproliferative activity because short treatments with the drug induce long-term effects *in vitro* and *in vivo*. To test that hypothesis, a total SCH 727965 dose of 260 mg/kg, equivalent to 20 mg/kg once daily for 13 days, was fractionated over several diverse schedules and administered to nude mice bearing established (>100 mm^3) A549 tumor xenografts (Fig. 3B; dosing days are indicated by arrows). Primary end points for this study were tumor volume/mass and body weight. SCH 727965 dosing of 87 mg/kg given once weekly exceeded the MTD and was terminated early. Similar tumor regressions were observed for all schedules. These data agree with earlier observations and indicate that similar *in vivo* responses can be generated on a wide range of intermittent SCH 727965 dosing schedules.

Mechanism-based systemic effects *in vivo* following exposure to SCH 727965

In this study, phospho-Rb 807/811 has been used as a surrogate marker of CDK engagement and mechanism-based SCH 727965 activity. To show that 20-mg/kg to 60-mg/kg doses of SCH 727965 previously exhibiting significant antitumor activity in a mouse xenograft model are associated with modulation of the CDK mechanism, the expression of phospho-Rb 807/811 was analyzed in skin samples taken from SCH 727965–treated, tumor-naïve nude mice. Skin and hair follicles are an excellent peripheral source of surrogate proliferating (nontumor) tissue. Skin punch biopsies were harvested at various time points following the administration of SCH 727965. Immunohistochemical staining of murine skin indicates that a single 40-mg/kg SCH 727965 dose induces rapid and sustained suppression of phospho-Rb 807/811 within the proliferating epithelial cells of the basal epithelium and hair follicles (Fig. 3C). These observations

Table 4. Dose dependent antitumor activity of SCH 727965

Compound (dose)	% MTD	% TGI
Paclitaxel (20 mg/kg, i.p., 2× weekly)	~50%	63%
SCH 727965 (8 mg/kg, i.p., QD)	13%	70%
SCH 727965 (16 mg/kg, i.p., QD)	27%	70%
SCH 727965 (32 mg/kg, i.p., QD)	53%	90%
SCH 727965 (48 mg/kg, i.p., QD)	80%	96%

Abbreviation: QD, once daily.

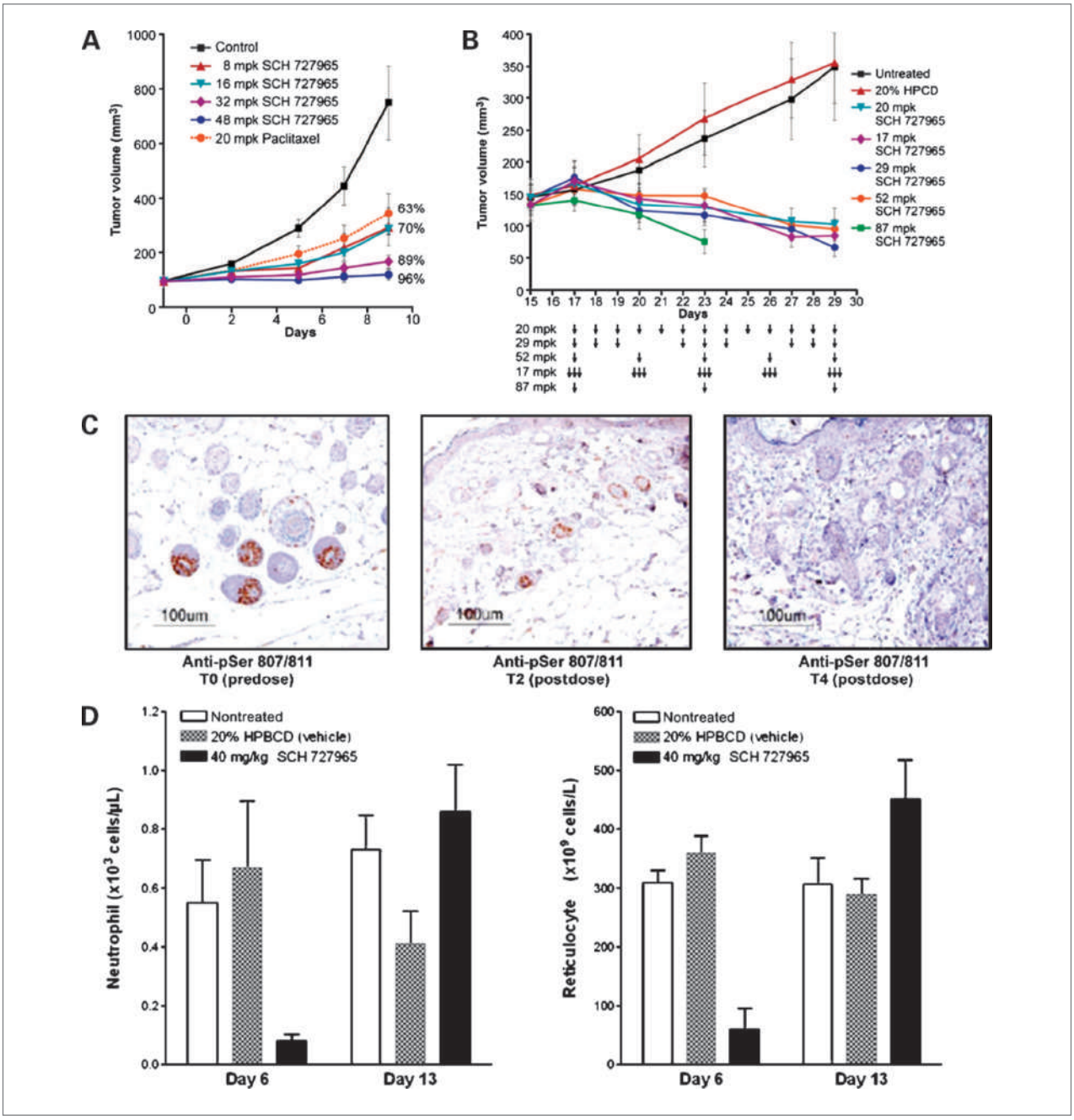

Figure 3. A, SCH 727965 efficacy in a mouse xenograft model. Nude mice inoculated s.c. with A2780 cells were treated with SCH 727965, paclitaxel, or vehicle control when tumor volume reached ~100 mm^3, ~7 d after inoculation. SCH 727965 was administered at 8, 16, 32, and 48 mg/kg i.p. daily for 10 d; paclitaxel was administered at 20 mg/kg i.p. twice weekly. Left, growth curves; right, percent tumor growth inhibition (%TGI) and percent of maximally tolerated dose (%MTD). B, SCH 727965 is active using intermittent dosing schedules in mice. A total dose equivalent to 20 mg/kg daily for 13 days (260 mg/kg) was fractionated over several diverse schedules and administered to nude mice bearing established A549 xenografts. SCH 727965 (87 mg/kg) exceeded the MTD (>20% body weight loss) when given on a once-weekly schedule. Similar regressions were observed on all schedules. C, SCH 727965 induces mechanism-based systemic effects *in vivo*. SCH 727965 induced rapid and sustained suppression of phospho-Rb within the proliferating epithelial cells of the basal epithelium and hair follicles. Skin samples were obtained from mice before treatment (T0, predose) or 2 and 4 h following administration of 40 mg/kg SCH 727965 i.p. (T2 and T4 postdose). Samples were stained with phospho-Rb Ser 807/811 specific antisera. D, SCH 727965 induces reversible hematologic effects. BALB/c mice were treated with SCH 727965 at 40 mg/kg on a dose-intense, daily for 5 days schedule. To determine blood cell count nadirs and reversibility, blood samples were obtained from mice on the day after the last SCH 727965 dose (day 6) and then 7 d later (day 13). Absolute neutrophil (left) and reticulocyte responses (right) are shown compared with BALB/c mice that were administered vehicle (20% hydroxypropyl-β-cyclodextran) or left nontreated. Neutrophil and reticulocyte nadirs were observed on day 6. By day 13, counts neutrophil and reticulocyte counts in SCH 727965–treated animals had returned to levels similar to those observed in vehicle-treated or nontreated mice. There were no detectable effects on platelets or RBC during the duration of this time course (data not shown).

suggest that doses of SCH 727965 associated with regressions in the A549 xenograft model (Fig. 3B) are correlated with the modulation of a mechanism-based marker in proliferating surrogate tissues. These data are consistent with the hypothesis that inhibition of CDKs can induce inhibition of cell cycle within proliferating normal tissues and suggest that proliferating compartments will likely be sensitive to SCH 727965.

To assess effects of SCH 727965 on hematologic parameters, BALB/c mice were i.p. dosed daily with 40 mg/kg for 5 days, with controls nontreated or dosed with a vehicle, 20% hydroxypropyl-β-cyclodextran. Blood samples were obtained 1 day after administration of the last dose (day 6) as well as 7 days later (day 13). Blood cells were counted (with differential) to examine nadir and rebound kinetics of several hematologic parameters. Neutrophils and reticulocytes were most sensitive to SCH 727965, and nadirs in their absolute counts were detected on day 6 (Fig. 3D). Significantly, absolute neutrophil counts (Fig. 3D, left) and reticulocyte counts (Fig. 3D, right) returned to normal levels by day 13. No detectable effects on platelets or RBC over this time course were observed (data not shown). These results are consistent with the mechanism-based activity of SCH 727965 within the examined dose range and suggest that cell cycle inhibition effects are transient and reversible in proliferating normal cell compartments.

Discussion

SCH 727965 was selected for clinical development following a functional *in vivo* screen that integrated both efficacy and tolerability of tested compounds. This rapid and discriminatory approach identified a candidate for clinical development that was significantly more effective and better tolerated than flavopiridol. SCH 727965 has several distinct *in vitro* properties consistent with an improved *in vivo* therapeutic index. Notably, the compound exhibits strong selectivity for the CDK family. These data suggest the activated CDK conformation has unique structural aspects, not present in closely related serine/threonine kinases (such as the extracellular signal-regulated kinase and GSK3 families), thus providing a potential explanation for the observed excellent selectivity and tolerability profiles of SCH 727965.

In vitro and *in vivo* analyses presented in this study support the conclusion that SCH 727965 has the potential to inhibit the growth of a broad spectrum of human cancers. SCH 727965 induced mechanism-based apoptosis in the vast majority of tested human tumor cell lines of diverse origin, following a single exposure. In agreement, SCH 727965 was effective at doses below the MTD level in multiple *in vivo* models and induced regression in several xenografts using continuous or intermittent schedules. Under similar conditions, the observed xenograft efficacy profiles of SCH 727965 were consistently superior to those achieved using approved benchmark agents, such as taxanes. Moreover, in mechanism-based biomarker studies, effective doses of the drug were sufficient to suppress phosphorylated Rb levels in surrogate tissues, such as skin and hair follicles. Likewise, active dose levels in the mouse were also associated with reversible effects on hematologic parameters. Quantitative tracking of leukocyte cell counts may offer an additional approach for tracking mechanism-based pharmacodynamic effects of SCH 727965.

Interestingly, the *in vivo* activity of SCH 727965 observed in murine systems was readily detectable despite rapid clearance of the parent compound from mouse plasma, indicating that continual exposure to SCH 727965 was not necessary for activity *in vivo*. Consistent with this, short exposure to SCH 727965 can induce long-lasting pharmacodynamic effects *in vitro*. Thus, a 2-hour exposure to ≤500 nmol/L SCH 727965 was sufficient to suppress BrdUrd incorporation 24 hours later. Similarly, transient *in vitro* exposure to SCH 727965 induced suppression of Rb phosphorylation that was correlated with induction of apoptosis. Significantly, escalation of SCH 727965 exposure (≤30 μmol/L) did not augment apoptotic phenotypes, suggesting a relative lack of nonspecific or off-target cytotoxicity. Taken together, the available *in vitro* and *in vivo* data show that long-lasting therapeutic effects can be induced within sensitive cells following short exposures to SCH 727965. It is possible that selecting compounds for further development solely on the basis of pharmacokinetic parameters would not have facilitated selection of SCH 727965 for clinical development. In summary, the approach of *in vivo* screening in mice ultimately led to the selection of a compound with attractive biochemical and pharmacologic properties.

Inhibitors of the CDK family have been proposed as attractive drug targets and pursued for oncology indications for several years, and several candidate molecules have entered clinical studies. In the case of flavopiridol, a combination of suboptimal selectivity, poor drug-like qualities, and adverse side effects may ultimately obscure any potentially desirable mechanism-based activities of this agent. In this study, we have described the novel pharmacologic properties of SCH 727965, a highly potent and selective CDK inhibitor that is differentiated from first generation CDK inhibitor compounds, such as flavopiridol. SCH 727965 is currently undergoing clinical testing against a range of solid and hematologic malignancies. The overall excellent profile of SCH 727965 suggests this molecule has the necessary properties to allow further pharmacologic exploration of the cell cycle mechanism in oncology.

Disclosure of Potential Conflicts of Interest

Authors are current/past employees of Schering-Plough/Merck and own shares or share options in Merck.

Received 04/12/2010; revised 05/18/2010; accepted 06/13/2010; published OnlineFirst 07/27/2010.

References

1. Sherr CJ. Growth factor-regulated G1 cyclins. Stem Cells 1994;12 Suppl 1:47–55; discussion -7.
2. Pines J. Protein kinases and cell cycle control. Semin Cell Biol 1994; 5:399–408.
3. Hall M, Peters G. Genetic alterations of cyclins, cyclin-dependent kinases, and Cdk inhibitors in human cancer. Adv Cancer Res 1996;68:67–108.
4. Sherr CJ. Cancer cell cycles. Science 1996;274:1672–7.
5. Hunter T, Pines J. Cyclins and cancer II: cyclin D and CDK inhibitors come of age. Cell 1994;79:573–82.
6. Ewen ME. The cell cycle and the retinoblastoma protein family. Cancer Metastasis Rev 1994;13:45–66.
7. Ewen ME. Regulation of the cell cycle by the Rb tumor suppressor family. Results Probl Cell Differ 1998;22:149–79.
8. Bregman DB, Pestell RG, Kidd VJ. Cell cycle regulation and RNA polymerase II. Front Biosci 2000;5:D244–57.
9. Oelgeschlager T. Regulation of RNA polymerase II activity by CTD phosphorylation and cell cycle control. J Cell Physiol 2002;190: 160–9.
10. van den Heuvel S, Harlow E. Distinct roles for cyclin-dependent kinases in cell cycle control. Science 1993;262:2050–4.
11. Hu B, Mitra J, van den Heuvel S, Enders GH. S and G2 phase roles for Cdk2 revealed by inducible expression of a dominant-negative mutant in human cells. Mol Cell Biol 2001;21:2755–66.
12. L'Italien L, Tanudji M, Russell L, Schebye XM. Unmasking the redundancy between Cdk1 and Cdk2 at G2 phase in human cancer cell lines. Cell Cycle 2006;5:984–93.
13. Cai D, Latham VM, Jr., Zhang X, Shapiro GI. Combined depletion of cell cycle and transcriptional cyclin-dependent kinase activities induces apoptosis in cancer cells 10.1158/0008-5472.CAN-06-1758. Cancer Res 2006;66:9270–80.
14. Gojo I, Zhang B, Fenton RG. The cyclin-dependent kinase inhibitor flavopiridol induces apoptosis in multiple myeloma cells through transcriptional repression and down-regulation of Mcl-1. Clin Cancer Res 2002;8:3527–38.
15. Chen R, Keating MJ, Gandhi V, Plunkett W. Transcription inhibition by flavopiridol: mechanism of chronic lymphocytic leukemia cell death 10.1182/blood-2005-04-1678. Blood 2005;106:2513–9.
16. Firestein R, Bass AJ, Kim SY, et al. CDK8 is a colorectal cancer oncogene that regulates [bgr]-catenin activity. 2008 2008/09/14/online.
17. Morris EJ, Ji J-Y, Yang F, et al. E2F1 represses [bgr]-catenin transcription and is antagonized by both pRB and CDK8. 2008 2008/09/14/online.
18. Chen YN, Sharma SK, Ramsey TM, et al. Selective killing of transformed cells by cyclin/cyclin-dependent kinase 2 antagonists. Proc Natl Acad Sci U S A 1999;96:4325–9.
19. Shapiro GI. Cyclin-dependent kinase pathways as targets for cancer treatment 10.1200/JCO.2005.03.7689. J Clin Oncol 2006; 24:1770–83.
20. Kummar S, Gutierrez M, Doroshow JH, Murgo AJ. Drug development in oncology: classical cytotoxics and molecularly targeted agents. Br J Clin Pharmacol 2006;62:15–26.
21. Paruch K, Dwyer MP, Alvarez C, et al. Discovery of dinaciclib (SCH 727965): a potent and selective inhibitor of cyclin-dependent kinases. ACS Med Chem Lett 2010. Epub ahead of print.